

## Three-dimensional microfabrication in bulk silicon using high-energy protons

E. J. Teo,<sup>a)</sup> M. B. H. Breese, E. P. Tavernier, A. A. Bettiol, and F. Watt

*Centre for Ion Beam Applications, Department of Physics, National University of Singapore, 2 Science Drive 3, Singapore 117542*

M. H. Liu and D. J. Blackwood

*Department of Materials Science, National University of Singapore, Singapore 117542*

(Received 24 October 2003; accepted 1 March 2004)

We report an alternative technique which utilizes fast-proton irradiation prior to electrochemical etching for three-dimensional microfabrication in bulk *p*-type silicon. The proton-induced damage increases the resistivity of the irradiated regions and acts as an etch stop for porous silicon formation. A raised structure of the scanned area is left behind after removal of the unirradiated regions with potassium hydroxide. By exposing the silicon to different proton energies, the implanted depth and hence structure height can be precisely varied. We demonstrate the versatility of this three-dimensional patterning process to create multilevel free-standing bridges in bulk silicon, as well as submicron pillars and high aspect-ratio nanotips. © 2004 American Institute of Physics. [DOI: 10.1063/1.1723703]

Many technologies, for example, nanoelectromechanical systems<sup>1–3</sup> and photonic crystals,<sup>4</sup> etc., require the fabrication of precise three-dimensional (3D) structures, preferably in silicon. One major limitation of conventional lithography and silicon etching technologies is the multiple processing steps involved in fabricating free-standing multilevel structures.<sup>1,2</sup> We report an alternative patterning process that utilizes fast-proton irradiation followed by electrochemical etching. This technique has the advantage that it can be used to fabricate multilevel free-standing microstructures in bulk silicon using a single etch step.

Electrochemical etching of silicon in hydrofluoric acid is a widely established technique for producing porous silicon with light emitting properties.<sup>5</sup> It is also emerging as an alternative technique for micromachining due to its low cost, fast etching process, and easy implementation. Porous silicon is often used as a sacrificial material to fabricate cavities or free-standing structures since it can be easily removed with potassium hydroxide (KOH) solution.<sup>6,7</sup> Selective patterning of porous silicon can be achieved through a mask or by etch stop techniques.<sup>8</sup> One drawback of using a mask is that the isotropic nature of the electrochemical etching process results in undercutting of the mask.<sup>9</sup> Anisotropy of the sidewalls can be improved with the use of a metallic mask as compared to a photoresist or SiO<sub>2</sub> mask. Lehmann and Foll<sup>10</sup> showed that the problem can be overcome by pre-structuring the masked surface in KOH solution to form a periodic array of etch pits before electrochemical etching. Due to the enhanced electric field, the holes are efficiently collected at the pore tips for etching. The depletion of holes in the space charge region prevents silicon dissolution at the sidewalls, enabling anisotropic etching of the trenches. This method is extensively used in *n*-type silicon to create very high aspect-ratio trenches.<sup>11–13</sup> Kleimann expanded the capability of the

technique to make free-standing structures such as micro-needles and tubes.<sup>14</sup>

Macropore formation in *p*-type silicon is more difficult than in *n*-type silicon because there is no space-charge region to control the diffusion of holes to the pore tips for anisotropic dissolution of silicon, and passivation of pore walls against dissolution. Another disadvantage of this approach is that a spatial periodicity is required for anisotropic etching.

Patterning of porous silicon using selective doping can be performed by low-energy boron, phosphorus or gallium ion implantation followed by high temperature annealing.<sup>15,16</sup> Based on the etching selectivity between *n*- and *p*-type silicon, patterned silicon microstructures can be obtained. In this letter, we employ a different etch-stop technique which relies on the localized damage created by a high dose of focused mega-electron-volt (MeV) proton irradiation for 3D microfabrication. A postirradiation annealing step is not needed in this case. As a 2 MeV proton penetrates the material, it loses energy and eventually comes to rest after traversing about 48 μm below the surface. Silicon vacancies are created along the ion path, with most of the damage produced at the end of range. According to stopping and range of ions in matter calculations,<sup>17</sup> a dose of 5 × 10<sup>15</sup> protons/cm<sup>2</sup> at an energy of 2 MeV will introduce a defect concentration of ~10<sup>19</sup> vacancies/cm<sup>3</sup> close to the surface, increasing sharply to a maximum of ~10<sup>20</sup> vacancies/cm<sup>3</sup> at the end of range, as shown schematically in Fig. 1(a). This is much higher than the dopant concentration of 5 × 10<sup>15</sup> B/cm<sup>3</sup> in the *p*-type sample used. Under anodic bias, the high density of proton-induced defects efficiently traps or recombines with the migrating holes. The resistivity of the irradiated regions is expected to increase by 3–4 orders of magnitude.<sup>18</sup> This significantly reduces the current flow through the damaged volume to the silicon-electrolyte interface [Fig. 1(a)], preventing the formation of porous silicon in the irradiated regions patterned by

<sup>a)</sup>Author to whom correspondence should be addressed; electronic mail: phytej@nus.edu.sg

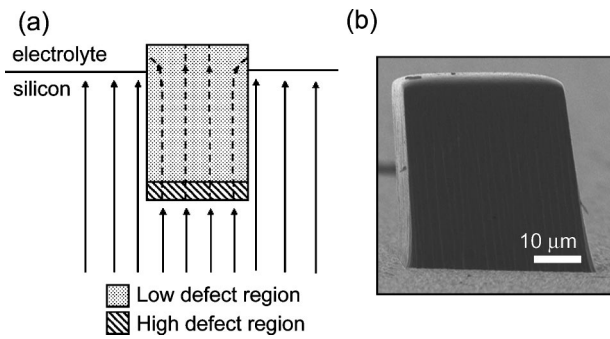


FIG. 1. (a) Diagram showing the reduced current flow (dashed lines) through a damaged region created by the ion beam. (b) Square structure obtained by 2 MeV proton irradiation with a dose of  $5 \times 10^{15}$  protons/cm<sup>2</sup>.

the proton beam. Since the MeV proton beam follows an almost straight path in the material with small lateral straggling, it is possible to obtain structures with vertical sidewalls, as seen in Fig. 1(b). This overcomes the undercutting effect encountered when a surface mask is used.<sup>9</sup> The high penetration depth of MeV protons in silicon also enables the production of much deeper structures compared to that produced by selective doping technique.

Figure 2 shows schematics of the process for silicon microfabrication. The feasibility of patterning with focused proton beams was first demonstrated by Polesello *et al.*,<sup>17</sup> though the resulting micromachined structures lacked edge definition and height due to the poor beam stability and spatial resolution. Also, the *p*-type silicon substrate was very heavily doped (15 mΩ cm), making it difficult to introduce enough defects to stop the high density of migrating holes. In this work, (100) *p*-type silicon with nominal resistivity of 15 Ω cm was used for micromachining. The proton irradiation was carried out using a high brightness, 3.5 MV single-ended accelerator.<sup>19</sup> A minimum beam resolution of 35 nm has been attained with our current proton beam writing facility.<sup>20</sup> Patterns were created by selectively scanning a 2 MeV proton

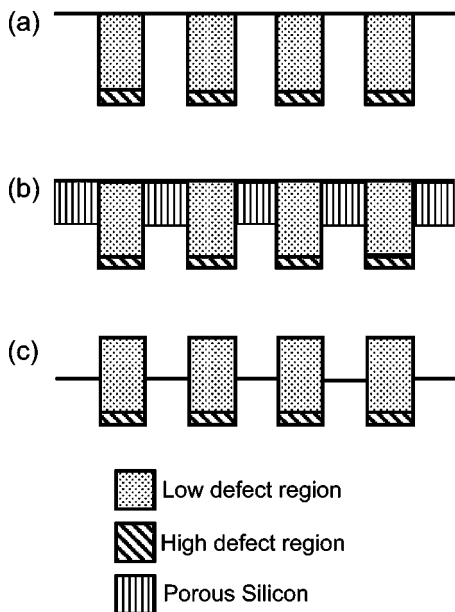


FIG. 2. (a) Patterning of *p*-type silicon with proton beam writing, (b) electrochemical etching to selectively form porous silicon in unirradiated regions, and (c) removal of porous silicon with diluted KOH solution.

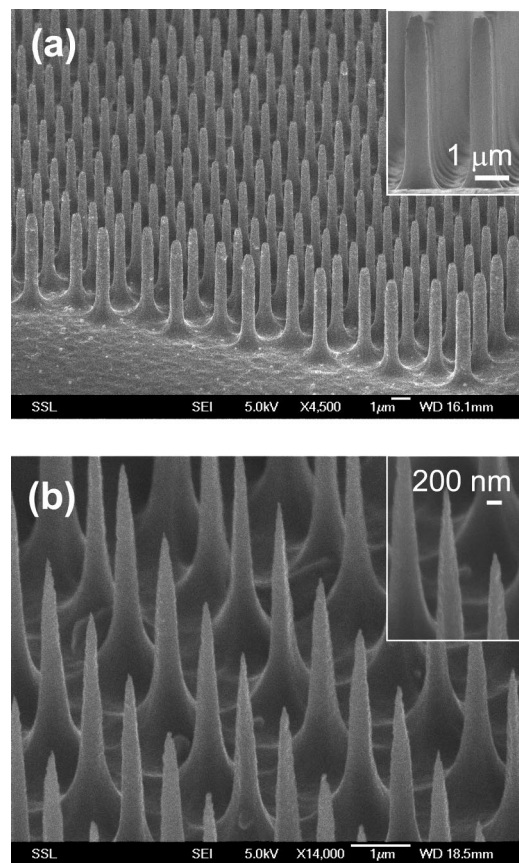


FIG. 3. (a) Array of high aspect-ratio pillars obtained by single spot irradiations. Inset picture shows the profile of the pillars. (b) Sharp spikes obtained when the beam is channeled along the  $\langle 100 \rangle$  crystal axis. Close-up SEM of the tip in the inset picture.

beam of 200 nm resolution across the *p*-type silicon [Fig. 2(a)]. The irradiated wafer was then electrochemically etched in an electrolyte mixture of HF:water:ethanol (1:1:2) [Fig. 2(b)]. Ethanol was added to reduce surface tension and wet the surface of porous silicon, thereby allowing hydrogen gas formed from the dissolution to escape. After etching, the porous silicon was removed by dipping the sample into diluted KOH solution for about 2–4 min. The final patterned structure on the wafer surface is a three-dimensional representation of the scanned pattern area [Fig. 2(c)]. The height of the microstructure is controlled by the etching time. The etch depth is determined from the height difference between the unetched and etched region by using a surface profilometer.

Figure 3(a) shows a scanning electron micrograph (SEM) of a uniform array of closely packed, high aspect-ratio pillars obtained by single spot irradiations of a focused proton beam. Each spot has an accumulated dose of  $5 \times 10^{16}$  protons/cm<sup>2</sup>. The sample was then etched for 15 min with a current density of 40 mA/cm<sup>2</sup>. The pillars are 4.5 μm high with a diameter of 0.6 μm, and a periodicity of 2 μm. The profile of the pillar reveals vertical and smooth sidewalls with slight broadening at the base. A longer etching time may be used to increase the height and aspect ratio of the silicon pillars. Such a periodic array of submicron diameter pillars is potentially important for the fabrication of photonic crystals.<sup>21</sup>

By aligning the incident ion beam with an axis or set of

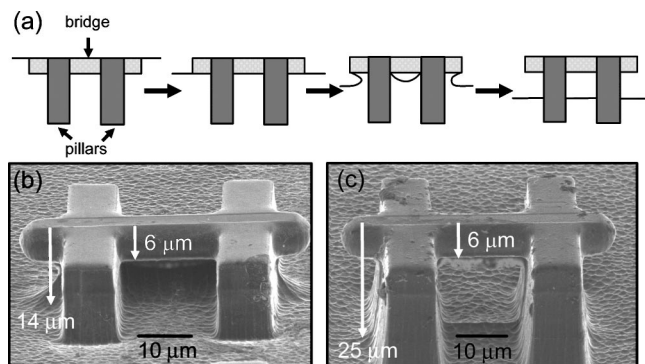


FIG. 4. (a) Evolution of the double-energy irradiated structure with etching depth. (b) At etch depth of  $14\ \mu\text{m}$ , the bridge starts to separate from the substrate. (c) The bridge is completely free standing at an etch depth of  $25\ \mu\text{m}$ .

crystal planes, the ion beam becomes channeled, which reduces the probability of nuclear collisions with silicon atoms.<sup>22</sup> This results in a significant reduction of the damage caused by the channeled ion beam close to the surface. Figure 3(b) shows the structure obtained with a similar irradiation pattern and dose as for the random structure in Fig. 3(a) but with the beam channeled along the  $\langle 100 \rangle$  axis of the sample. The reduced damage created near the surface regions results in much sharper and thinner tips, with a radius of curvature of about  $15\ \text{nm}$  at the tip, sloped steeply at an angle of  $85^\circ$  [Fig. 3(b) inset]. These nanotips can be used in applications such as scanning probe microscopes or field emission array. Recently, there has been an increasing interest in using atomic force microscope (AFM) tips for nanolithography,<sup>23</sup> through deposition of molecule clusters. The multiple assemblies of uniform nanotips can allow for the mass transport of dots of molecules onto the substrate.

After prolonged etching beyond the end of range, the isotropic etching process starts to undercut the structure. This means that multilevel structures can be created by exposing the sample with two different proton energies. Since the structure irradiated with lower energy has a shorter range, it will begin to undercut at a shallower etch depth while the structure with higher energy irradiation continues to increase in height. In this way, we can fabricate multi-level free-standing microstructures in a single etch step. This would have required multiple processing steps if a conventional lithography technique was used. To demonstrate this capability, a bridge structure was irradiated with  $0.5\ \text{MeV}$  protons, and two supporting pillars with  $2\ \text{MeV}$  protons. Figure 4(a) shows the progress of the subsequent etching process that led to a formation of the free-standing bridge. Initially, etching occurs in all regions except the irradiated portions. As the etching goes beyond the end of range of  $0.5\ \text{MeV}$  protons ( $\sim 6\ \mu\text{m}$ ), undercutting of the bridge starts to occur. At an etch depth of  $14\ \mu\text{m}$ , the SEM picture in Fig. 4(b) shows that the bridge is fully undercut and separates from the substrate. It remains supported by the two pillars irradiated by higher energy. The structure of a free-standing bridge is formed af-

ter further etching to  $25\ \mu\text{m}$  below the surface [Fig. 4(c)]. Undercutting does not occur at the pillars as the range of  $2\ \text{MeV}$  protons is  $48\ \mu\text{m}$ . The much smoother surface of the irradiated structures as compared to the unirradiated regions suggests that porous silicon is strongly restricted from forming in the irradiated regions. AFM measurements show that the root-mean-square roughness of  $8\ \text{nm}$  in the irradiated surface is similar to that of un-etched silicon.

In conclusion, we demonstrate the ability to overcome the isotropic nature of the electrochemical etching process to produce high aspect-ratio pillars by bulk patterning of silicon with  $\text{MeV}$  protons. With multiple energy exposures, the structure height can be precisely controlled to obtain free-standing multilevel microstructures using a single etch step. Combined with the high spatial resolution of the proton beam, this technique opens up new possibilities for precise 3D microfabrication of silicon in a direct and flexible way.

E. J. Teo acknowledges the financial support by Singapore Millennium Foundation. The authors are grateful to J. A. van Kan for setting up the high resolution ion beam line.

- <sup>1</sup>H. G. Craighead, *Science* **290**, 1532 (2000).
- <sup>2</sup>A. N. Cleland and M. L. Roukes, *Appl. Phys. Lett.* **69**, 2653 (1996).
- <sup>3</sup>J. Fritz, M. K. Baller, H. P. Lang, H. Rothuizen, P. Vettiger, E. Meyer, H.-J. Guntherodt, Ch. Gerver, and J. K. Gimzewski, *Science* **288**, 316 (2000).
- <sup>4</sup>S. Y. Lin, J. G. Fleming, D. L. Hetherington, B. K. Smith, R. Biswas, K. M. Ho, M. M. Sigalas, W. Zubrzycki, S. R. Kurtz and Jim Bur, *Nature (London)* **394**, 251 (1998).
- <sup>5</sup>L. T. Canham, *Appl. Phys. Lett.* **57**, 1046 (1990).
- <sup>6</sup>M. Navarro, J. M. Lopez-Villegas, J. Samitier, J. R. Morante, J. Bausells, and A. Merlos, *J. Micromech. Microeng.* **7**, 131 (1997).
- <sup>7</sup>T. E. Bell, P. T. J. Gennissen, D. DeMunter, and M. Kuhl, *J. Micromech. Microeng.* **6**, 361 (1996).
- <sup>8</sup>A. G. Nassiopoulou, in *Properties of Porous silicon*, edited by L. Canham, (INSPEC, London, 1997), No. 18 pp. 77–80.
- <sup>9</sup>P. Steiner and W. Lang, *Thin Solid Films* **255**, 52 (1995).
- <sup>10</sup>V. Lehmann and H. Foll, *J. Electrochem. Soc.* **137**, 653 (1990).
- <sup>11</sup>V. Lehmann, *J. Electrochem. Soc.* **140**, 2836 (1993).
- <sup>12</sup>F. Muller, A. Birner, U. Gosele, V. Lehmann, S. Ottow, and H. Foll, *J. Porous Mater.* **7**, 201 (2000).
- <sup>13</sup>H. W. Lau, G. J. Parker, R. Greef, and M. Holling, *Appl. Phys. Lett.* **67**, 1877 (1995).
- <sup>14</sup>P. Kleimann, J. Linnros, and R. Juhasz, *Appl. Phys. Lett.* **79**, 1727 (2001).
- <sup>15</sup>J. Xu and A. J. Steckl, *Appl. Phys. Lett.* **65**, 2081 (1994).
- <sup>16</sup>C. J. M. Eijkel, J. Branebjerg, M. Elwenspoek, and F. C. M. Van de Pol, *IEEE Electron Device Lett.* **11**, 588 (1990).
- <sup>17</sup>P. Polesello, C. Manfredotti, F. Fizzotti, R. Lu, E. Vittone, G. Lerondel, A. M. Rossi, G. Amato, L. Boarino, S. Galassini, M. Jaksic and Z. Pastuovic, *Nucl. Instrum. Methods Phys. Res. B* **158**, 173 (1999).
- <sup>18</sup>M. Yamaguchi, S. J. Taylor, M. J. Yang, S. Matsuda, O. Kawasaki, and T. Hisamatsu, *J. Appl. Phys.* **80**, 4916 (1996).
- <sup>19</sup>F. Watt, J. A. van Kan, A. A. Bettioli, T. F. Choo, M. B. H. Breese, and T. Osipowicz, *Nucl. Instrum. Methods Phys. Res. B* **210**, 14 (2003).
- <sup>20</sup>J. A. van Kan, A. A. Bettioli, and F. Watt, *Appl. Phys. Lett.* **83**, 1629 (2003).
- <sup>21</sup>T. Zijlstra, E. van der Drift, M. J. A. De Dood, E. Snoeks, and A. Polman, *J. Vac. Sci. Technol. B* **17**, 2734 (1999).
- <sup>22</sup>L. C. Feldman, J. W. Mayer, and S. T. Picraux, *Materials Analysis by Ion Channeling* (Academic, New York, 1982).
- <sup>23</sup>R. D. Piner, J. Zhu, F. Xu, S. Hong, and C. A. Mirkin, *Science* **283**, 661 (1999).